Original Article

DOI: 10.5582/ddt.2023.01057

Effects of plant-based copper nanoparticles on the elimination of ciprofloxacin

Tanongsak Sassa-deepaeng[1], Wachira Yodthong[2], Nattakanwadee Khumpirapang[3], Songyot Anuchapreeda[4,6], Siriporn Okonogi[5,6,*]

[1] Agricultural Biochemistry Research Unit, Faculty of Sciences and Agricultural Technology, Rajamangala University of Technology Lanna Lampang, Lampang, Thailand;
[2] Lampang Inland Fisheries Research and Development Center, Lampang, Thailand;
[3] Department of Pharmaceutical Chemistry and Pharmacognosy, Faculty of Pharmaceutical Sciences, Naresuan University, Phitsanulok, Thailand;
[4] Department of Medical Technology, Faculty of Associated Medical Sciences, Chiang Mai University, Chiang Mai, Thailand;
[5] Department of Pharmaceutical Sciences, Faculty of Pharmacy, Chiang Mai University, Chiang Mai, Thailand;
[6] Center of Excellence in Pharmaceutical Nanotechnology, Faculty of Pharmacy, Chiang Mai University, Chiang Mai, Thailand.

SUMMARY Ciprofloxacin (CIP) is frequently detected in the environment and causes the emergence of drug-resistant bacteria. High levels of CIP in the environment are also harmful to humans and animals. Therefore, effective elimination of CIP is required. In this study, plant-based copper nanoparticles (CuNPs) have been fabricated for the purpose of eliminating CIP. Aqueous extracts of 6 plants were compared for their phytochemicals and reducing activity. Among all the extracts, *Garcinia mangostana* extract (GM) was the most potent with the highest total phenolic compounds, flavonoids, tannins, terpenoids, and reducing activity. CuNPs synthesized using GM (GM-CuNPs) were characterized using UV-VIS spectroscopy and dynamic light scattering. The results showed that the maximum absorption of GM-CuNPs was at 340 nm. The average size of GM-CuNPs is in the nanoscale range of 159.2 ± 61 nm, with a narrow size distribution and a negative zeta potential of – 4.13 ± 6.97 mV. The stability of GM-CuNPs is not solely due to their zeta potential but also phytochemicals in the extract. GM-CuNPs at 25 mM showed the highest efficiency of 95% in removing CIP from aqueous medium pH 6-7 at 25-35°C within 20 min. The results indicated that the electrostatic attraction between the negative charge of GM-CuNPs and the positive charge of CIP controlled the drug adsorption on the nanoparticles. In conclusion, the developed GM-CuNPs have excellent CIP removal efficiency. These synthesized GM-CuNPs are expected to be environmentally friendly for the removal of antibiotics and other drugs.

Keywords *Garcinia mangostana*, eco-friendly, green synthesis, metal nanoparticles, plant extract

1. Introduction

It is known that many drugs in humans and animals are eliminated through urine and feces, and released into the wastewater system (*1*). Ciprofloxacin (CIP), one of the most widely used antibiotics for treatment of bacterial infections in both humans and animals, is secreted in the urine in its original form (*2*). Therefore, large amounts of CIP are found in wastewater systems. In addition, pharmaceutical manufacturers and hospitals are also the most important sources of contaminated wastewater. This leads to increase contamination in surface and groundwater, and is extremely harmful to the environment and human health (*3,4*). It has been reported that CIP contamination of daily drinking water can cause mild nausea, vomiting, headaches, and diarrhea. Higher CIP contamination can cause more serious adverse effects, such as thrombocytopenia and acute renal failure. Additionally, the presence of CIP in water supplies has resulted in the development of antibiotic-resistant bacteria (*5*), resulting in an increase in health problems. This is because treating drug-resistant bacteria is difficult, high cost, and requires different drug or a higher dose. Therefore, the effective removal of CIP is required. Technology using metal nanoparticles appears to be a convenient alternative (*6*) and promising for the removal of CIP by an adsorption mechanism (*7,8*). Several metal-based techniques have been developed to synthesize metal nanoparticles, such as chemical laser ablation, chemical reduction, coprecipitation, and wave-

assisted processes (*9,10*). However, these methods are expensive and not environmentally friendly. This is because many harmful by-products are released into the environment. The limitations of these methods have given rise to new technologies of plant-based synthesis, by biomolecules are used instead. Plant-assisted synthesis is environmentally friendly, cost effective, and can help overcome all limitations. It has been proven to be an effective and highly reliable technique in preparing metal nanoparticles. However, to obtain the desired metal nanoparticles by plant-based synthesis, it is necessary to use biomaterial with high reducing power. Several reports indicate that certain plant-derived phenolic compounds such as flavonoids and tannins possess antioxidant activity and reducing power. In this study, the phytochemical contents of 6 potential plant extracts, *Ageratum conyzoides*, *Emilia sonchifolia*, *Garcinia mangostana*, *Sesbania grandiflora*, *Tridax procumbens*, and *Xanthium strumarium* were compare and the most effective plant extract was selected for synthesis of copper nanoparticles (CuNPs).

A. conyzoides, an allelopathic plant in the family Asteraceae, is a good source of antioxidants due to its high content of total phenolic compounds and flavonoids (*11*). Different parts of this plant have been used in folk medicine for decades. *E. sonchifolia*, *T. procumbens* and *X. strumarium* are members of the Asteraceae family. *E. sonchifolia* has previously been reported to inhibit the formation of hydroxyl radicals and superoxide radicals (*12*). Its major active ingredient is emiline, which is an alkaloid with antioxidant potential and neuroprotective effect against corticosterone-induced apoptosis in cancer cell lines (*13*). Up to date, there are no reports of using this compound as a reducing agent in the production of metal nanoparticles. Therefore, it remains a challenge as a primary plant in this experiment. *T. procumbens* contains alkaloids, carotenoids, flavonoids, fatty acids, steroids, phytosterols, tannins, and has high antioxidant activity (*14*). *X. strumarium* has been reported to have high antioxidant activity and reducing power (*15*). The antioxidant properties of this plant are related to the levels of alkaloids, phenolic acids, diterpenes, saponins, glycosides, essential oils and phytosterols (*16,17*). *G. mangostana* is a tropical perennial with edible fruits. It belongs to the Guttiferae family. This plant has been used in traditional and folk medicine systems in Southeast Asia to treat cystitis, dysentery, gonorrhea, inflammatory skin and abnormalities of urinary tract and to increase the efficiency of wound healing (*18*). It has been documented as a reducing agent for the fabrication of metal nanoparticles due to its phytochemical composition in the aqueous extract (*19*). *S. grandiflora,* which belongs to the family Leguminoseae, is an important agroforestry as a food source for humans, cattle, and goats in Thailand. Its bark extract possesses strong antibacterial activity (*20*). Antioxidant activity and the use in the plant-based synthesis of silver nanoparticles from this plant have also been reported (*21*). The main objective of this study was to synthesize CuNPs for the elimination of CIP. In this synthesis, a green biosynthesis method was used. The most effective plant extracts from these six potential plants were used as reducing agents. The synthesized CuNPs were studied for their physicochemical characterization and CIP removal efficiency in various water conditions.

2. Materials and Methods

2.1. Materials

Copper sulfate pentahydrate, ferric chloride, potassium ferricyanide, sodium nitrate and sodium nitrite were purchased from Ajax Finechem (New South Wales, Australia). CIP hydrochloride and gallic acid were from Bio Basic Inc. (Markham, Canada). Epigallocatechin gallate, quercetin, and 2,2-diphenyl-1-picrylhydrazyl hydrate (DPPH) were from Sigma-Aldrich (Steinheim, Germany). Hydrochloric acid (HCl) was from QRëC (Auckland, New Zealand. Folin-Ciocalteu reagent was from Loba Chemie (Mumbai, India). Aluminum chloride hexahydrate, bromophenol blue, and calcium carbonate were from Kemaus (New South Wales, Australia). Trichloroacetic acid and vanillin were from Merck (Damstadt, Germany). Sodium hydroxide (NaOH) was from RCI Lab-scan (Bangkok, Thailand). All other solvents and chemicals were of analytical grade.

2.2. Plants and extract preparation

A. conyzoides, *E. sonchifolia*, *G. mangostana*, *S. grandiflora*, *T. procumbens* and *X. strumarium* were collected from northern Thailand during July-December 2021. The plants were authenticated by herbalists from Rajamangala University of Technology Lanna, Thailand. All specimens are preserved at the university's herbarium. Fresh leaves of each plant were detached from the stems and washed thoroughly with tap water and deionized water, respectively. After that, the whole leaf material was dried in a hot air oven at 50°C until a constant weight was achieved. Then pulverized with an electric blender. The plant powder sieved through a 20-mesh sieve was vacuum-wrapped in a plastic bag and stored in a deep freezer at –20°C for further use.

To prepare the aqueous extract of each plant, 100 mg of dried plant powder was boiled with 10 mL of distilled water at 85°C for 30 min. Afterwards, the mixture was cooled to room temperature. It was then filtered through a 0.22-micron nylon syringe filter. The obtained filtrate was used for further studies.

2.3. Phytochemical studies

Freshly prepared aqueous extracts of each plant were

examined for total phenolic content (TPC), flavonoids and tannins. TPC content was determined by mixing 20 µL of the extract with 100 µL Folin-Ciocalteu reagent in 1,980 µL deionized water. After 5 min of incubation, 300 µL of 7% sodium nitrate solution was added and mixed well. The resulting mixture was further incubated for 60 min in the dark at room temperature. It was then measured for the absorbance at 765 nm. TPC was determined using a calibration curve made from various concentrations of gallic acid and expressed as µg of gallic acid equivalent (GAE) per mg of extract.

The total flavonoid content (TFC) of the samples was determined by mixing 20 µL of extract with 380 µL deionized water, then 100 µL of 5% sodium nitrite solution was added. After 5 min of incubation, the mixture was added with 100 µL of 10% aluminum chloride solution and allowed to stand for 6 min at room temperature. Finally, 400 µL of 1M NaOH solution was added. After completion of 15 min of incubation in the dark, absorbance was measured at 415 nm. TFC was determined using a calibration curve generated from quercetin at various concentrations and expressed as µg quercetin equivalent (QE) per mg of extract.

For determination of total tannin content (TTC), 250 µL of extract was vigorously shaken with 450 µL of 1% vanillin reagent. After 5 min of incubation, the mixture was mixed with 300 µL of concentrated HCl and then was incubated for 30 min at ambient temperature. Finally, the color of the solution changed to red. The absorbance was measured at 500 nm. TTC was determined using a calibration curve generated from epigallocatechin gallate at various concentrations and expressed as µg of epigallocatechin gallate equivalent (EE) per mg of extract.

2.4. Determination of reducing power

High reducing power is an important factor in the production of metal nanoparticles. Measurement of the reducing potential of plant extracts was performed using an assay according to a previously described method (*22*) with some modifications. Briefly, the diluted concentration of each extract (12.5, 25, 50 and 100 µg/mL) and the standard antioxidant, gallic acid was mixed with 1.0 mL of 0.2 M sodium phosphate buffer (pH 6.6) and 1.0 mL of 1% potassium ferricyanide. After vigorously shaking, the mixture was incubated at 50°C in a dry bath for 20 min, then 1.0 mL of 10% trichloroacetic acid was mixed and centrifuged at 4,000 rpm for 10 min. An aliquot of 0.5 mL of supernatant was diluted with the same volume of distilled water. Finally, 50 µL of 0.1% ferric chloride was added. After incubation for 10 min, the absorbance was determined at 700 nm against a reagent blank. Distilled water was used as a blank. The reducing power was determined using a calibration curve made from gallic acid at various concentrations and expressed as µg of GAE per mg of extract.

2.5. Synthesis of CuNPs

The synthesis of CuNPs was conducted according to a previously described method (*23*) with some modification. Briefly, copper sulfate was dissolved in deionized water to obtain a final concentration of 50 mM. After that, 200 µL of extract and 300 µL of deionized water were vigorously mixed with 500 µL of copper sulphate solution prior to refluxing at 80°C for 30 min in a dry incubator to stimulate the reduction of metal salt. The color of the dispersion gradually changed from colorless to yellow and then to dark orange. This indicates the formation of particles in the nanoscale range (*24*). The solution was allowed to cool to ambient temperature and used for further studies.

2.6. Characterization of CuNPs

The formed CuNPs was characterized using a V-1200 spectrophotometer with UV-Professional analysis software (Dshing Instrument Co., Ltd., ZhuHai, China). The UV-visible spectrum of CuNPs enclosed in 1.5 mL disposable PMMA cuvettes (BRAND GmbH & Co. KG, Wertheim, Germany) was detected in the wavelength range 320 to 800 nm, operating at a resolution of 5 nm. The extracts and copper sulfate solution were also examined under the same conditions.

The lyophilized CuNPs were resuspended in 1 mL deionized water. The size and size distribution (PdI) as well as zeta potential of CuNPs were determined using a Nano-ZS zetasizer (DTS 1060, Malvern Instruments Ltd., Worcestershire, UK) based on the principle of dynamic light scattering (*25,26*). The results were automatically calculated by the software according to the instrument manufacturer's recommendations.

2.7. Removal efficiency of CuNPs

In this experiment, CuNPs synthesized using selected plant extracts were used. The CIP removal efficiency (CRE) of the synthesized CuNPs was examined using the CIP solutions. For the preparation of CIP solution, 25 mg of CIP hydrochloride was dissolved in 100 mL of distilled water. Factors that might affect CRE include: CuNPs concentration, contact time, pH, and temperature were mornitored. To study the effects of pH, the pH of the tested solution was adjusted by adding 0.1 N HCl or 0.1 N NaOH to achieve a pH range of 3-10.

The selected CuNPs colloidal dispersion was mixed with freshly prepared CIP sample solution and kept at room temperature for 60 min. The samples were collected at different time intervals and centrifuged at 500 rpm for 10 min. An aliquot of 250 µL of the supernatant was mixed with 100 µL of 20 mM acetate buffer, pH 4.1, and 375 µL of 0.1% bromophenol blue. After incubation at room temperature for 10 min, 2.5 mL of chloroform was added and the mixture

was shaken vigorously for 30 s, which resulted in the separation between chloroform and water. The yellow layer was determined at 416 nm relative to the blank. Calibration curves were generated by diluting CIP to various concentrations (R^2 = 0.99). The CIP content was expressed in µg. The system without CuNPs was used as a control. CRE can be calculated using the following equation: CRE (%) = [(*Ac* – *As*)/*Ac*] × 100, where *Ac* is the absorbance of the control and *As* is the absorbance of the sample.

2.8. Statistical analysis

All experiments were carried out in triplicate. The obtained data were analyzed using Microsoft Excel 2016 for Windows and presented as mean ± standard deviation (SD). The data were analyzed by one-way ANOVA and Duncan's mean comparison test at the 5% significance level.

3. Results

3.1. Phytochemicals and reducing power of extracts

The phytochemical content and reducing power of the extracts of the six plants are shown in Table 1. It can be clearly seen that the *G. Mangostana* extract had the highest TPC, TFC, and TTC with the GAE, QE, and EE values of 98.86 ± 1.20 mg/g, 109.22 ± 4.06 mg/g, and 209.67 ± 7.29 mg/g, respectively. This extract was selected for further studies.

3.2. CuNPs synthesis and particle characterization

G. mangostana extract was used as a reducing agent in the synthesis of CuNPs, and the obtained CuNPs were named as GM-CuNPs. The blue color of the copper sulfate solution changed to light brown after boiling the mixture at 80ºC for 30 min. The different appearance and color of GM-CuNPs colloidal system are shown in Figure 1. After characterization, the results confirmed that the particle size of GM-CuNPs was in the nanoscale range with an average diameter of 159 ± 61 nm and a narrow PdI value of 0.280 ± 0.003. GM-CuNPs were also found to have a negative surface charge with a zeta potential of – 4.13 ± 6.97 mV.

3.3. Effect of GM-CuNPs concentration on CIP removal

In this study, aqueous medium, pH 7, containing CIP at a concentration 0.25 g/L was treated with GM-CuNPs at concentrations ranging from 0.20 to 100 mM for 60 min at room temperature. The results as shown in Figure 2, indicate that the removal efficiency increased with the increase in the concentration of the synthesized GM-CuNPs. An increase in CIP removal capacity was observed from a CRE value of 24.1% to 98.2% when the GM-CuNPs concentration increased from 0.20 mM to 100 mM. The removal efficiency was highest when the concentration of GM-CuNPs was 25 mM. From these results, GM-CuNPs at a concentration of 25 mM was considered the most effective concentration to remove CIP and was selected for further study.

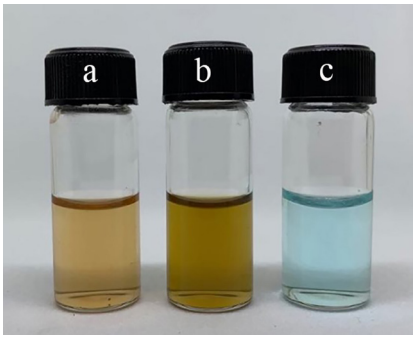

Figure 1. Appearance and color of *G. mangostana* extract solution (a), GM-CuNPs colloidal system (b), and copper sulfate solution (c).

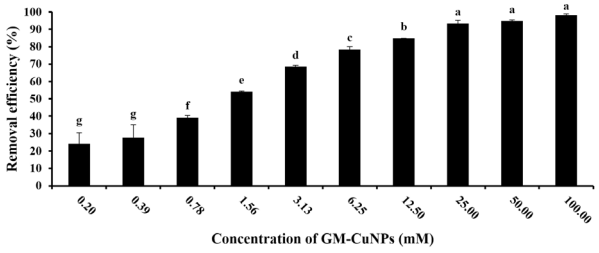

Figure 2. Effect of GM-CuNPs concentration on CIP removal efficiency. Different letters indicated statistically significant values ($p < 0.05$).

Table 1. Phytochemical properties and reducing power of the extracts

Plants	TPC	TFC	TTC	Reducing power
A. conyzoides	44.88 ± 0.37^{b}	42.19 ± 0.45^{b}	13.78 ± 0.85^{b}	234.61 ± 4.25^{b}
E. sonchifolia	24.05 ± 0.84^{c}	21.49 ± 0.61^{c}	2.87 ± 0.15^{c}	92.98 ± 3.92^{d}
G. mangostana	98.86 ± 1.20^{a}	109.22 ± 4.06^{a}	209.67 ± 7.29^{a}	358.82 ± 2.34^{a}
S. grandiflora	18.12 ± 1.20^{e}	21.78 ± 1.73^{c}	1.79 ± 0.60^{c}	41.61 ± 2.79^{f}
T. procumbens	15.73 ± 0.21^{f}	14.19 ± 0.60^{d}	6.84 ± 2.33^{c}	75.45 ± 3.21^{e}
X. strumarium	21.40 ± 0.16^{d}	23.63 ± 0.70^{c}	7.49 ± 0.26^{c}	121.82 ± 0.08^{c}

Data present mean ± standard deviation of triplicate analysis. Different lowercase letters in the same column indicate statistically significant values ($p < 0.05$).

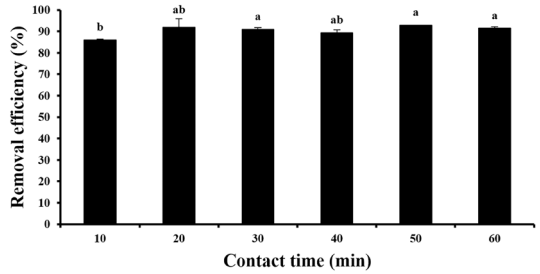

Figure 3. Effect of exposure time on CIP removal efficiency. Different letters indicate statistically significant values ($p < 0.05$).

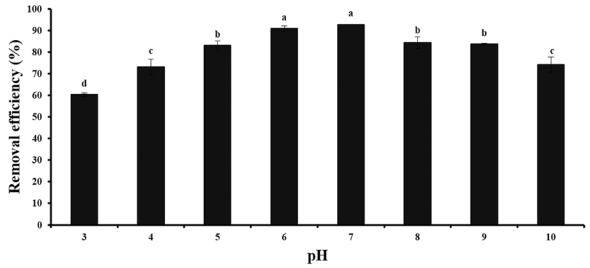

Figure 4. Effect of pH on CIP removal efficiency. Different letters indicate statistically significant values ($p < 0.05$).

3.4. Effect of exposure time

Exposure period between GM-CuNPs and CIP for different time intervals (10, 20, 30, 40, 50, and 60 min) was studied using GM-CuNPs at a concentration of 25 mM in medium at pH 7.0 and at room temperature. CRE values were found to increase with increasing exposure time. As shown in Figure 3, the CRE value at an exposure time of 10 min was 86.0 ± 0.7%. Then, as the exposure time increased, the CRE value gradually increased to 91.8 ± 1.1% at an exposure time of 60 min. It is seen that CIP was rapidly removed by GM-CuNPs and achieved the highest removal efficiency in the first 20 min and then reached equilibrium.

3.5. Effect of pH

We hypothesized that pH might be another important factor for controlling the CIP removal process of GM-CuNPs. Therefore, the synthesized GM-CuNPs were added to the CIP aqueous solutions at various pH ranges of 3-10 to obtain a final concentration of 68 mM CIP and 25 mM GM-CuNPs. The results showed that the removal efficiency of GM-CuNPs at different pH was different as shown in Figure 4. It was found that increasing the pH value from 3.0 to 6.0 could increase the percentage of CRE from 60.4% to 92.8%, respectively. The highest CRE value in 20 min contact was obtained in the pH range of 6-7. However, when the pH was further increased, it was found that the efficiency of removal decreased.

3.6. Effect of temperature

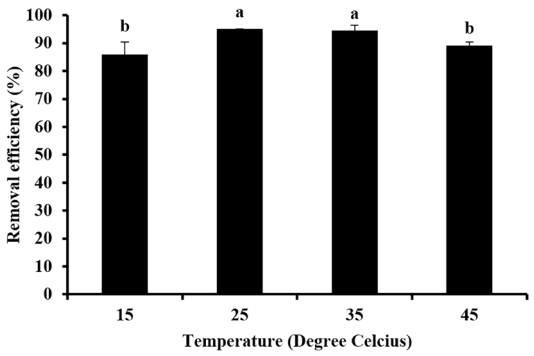

Figure 5. Effect of temperature on CIP removal efficiency. Different letters indicate statistically significant values ($p < 0.05$).

CIP removal efficiency by GM-CuNPs at various temperatures are presented in Figure 5. The results showed that the CIP removal efficiency was highest at the temperature range of 25-35°C (with CRE of 95.1 and 94.5%) and slightly decreased at 15°C and 45°C (with CRE of 85.9 and 89.2%).

4. Discussion

Flavonoids and tannins are important phytochemical groups. The principle chemical structure of flavonoids consists of two phenyl rings connected by a linear three-carbon bond (*27*). Flavonoids are classified according to their substituents and the oxidation state of the heterocyclic ring into flavones, isoflavones, flavanones, flavanols, and anthocyanidin (*28*). Tannins are bitter nitrogen-free polyphenolic compounds that have a bitter taste. Their molecular weight ranges between 500 to 20,000. Tannins can be divided into two groups: condensed tannins or non-hydrolysable tannins such as proanthocyanidins and hydrolysable tannins such as catechin and gallic acid (*29*). Both flavonoids and tannins possess various pharmacological effects, such as antioxidant, antiviral, antibacterial, and anti-inflammatory properties (*28,30*). It has been reported that the antioxidant effects of these polyphenolic compounds are due to H-atom transfer or single-electron transfer mechanisms (*31,32*). Therefore, these phenolic compounds have significant impact on the reducing properties of the sample, and affect the redox reactions of metal nanoparticles formulation (*33,34*). The results confirm that among the six plant extracts, *G. Mangostana* extract possessed the highest TPC, TFC, and TTC, and the highest reducing power. Therefore, this extract was selected for nanometal preparation.

During synthesis, the color of copper sulfate solution transformed from blue to light brown, confirming that all Cu^{2+} were reduced to Cu^{0} and GM-CuNPs were completely formed. The color of the obtained CuNPs colloidal systems is due to the fluctuation of the surface plasmon excitation in CuNPs. A wide range of colors was observed after the formation of CuNPs

was completed. This variation can be caused by several factors, including reaction time and temperature. In addition, one of the most important factors is the type of reducing agent. It has been reported that when ascorbic acid (*35*) and *Fortunella margarita* extract (*36*) were used as a reducing agent, the colors of the obtained CuNPs colloidal systems were yellow-brown and yellowish-green, respectively. The current study used *G. Mangostana* extract, which has a different color from the two reducing agents reported above. Therefore, the color of colloidal GM-CuNPs obtained was light brown. However, these color changes are useful in indicating the complete formation of CuNPs. The maximum absorbance of the synthesized CuNPs is in the range approximately 320-370 nm. High absorbance indicates a high conversion of Cu^{+2} to Cu^{0} and results in a high concentration of CuNPs (*37*). Consistent with previously reported (*38*), they found that an absorption peak of 370 nm was observed when *Cissus vitiginea* extract was used. In the present study, the absorbance of the synthesized CuNPs was 340 nm, which is consistent with CuNPs synthesized using curry leaf extract (*39*). The particle size of GM-CuNPs was in the nanoscale range with a narrow size distribution similar to that synthesized using the aqueous extract of *Carica papaya* leaves as a reducing agent and copper sulfate as a precursor (*40*). The zeta potential is an important parameter for predicting the stability of particles in colloidal systems. In general, a zeta potential of ± 30 mV is sufficient to prevent particles from coalescing by electrostatic repulsion (*41*). Zeta potential values near zero indicate weak repulsive forces between particles. This results in the agglomeration of particles. Interestingly, although the zeta potential values of the synthesized CuNPs using various plant extracts were close to zero (*42-44*), the obtained metal nanoparticles still did not aggregate. It has been reported that some phytochemicals present in plant extracts play important roles not only as reducing agents but also particle stabilizing agents (*45*). Therefore, the nanoparticles can be prevented from agglomeration, and the obtained CuNPs are stable despite their low zeta potential.

Our results show that the concentration of GM-CuNPs affects the removal efficiency. It has been reported that the addition of the nanoparticles increases the number of available adsorption sites (*46*), thus resulting in an increase in CRE. The present study shows that CIP was rapidly eliminated by GM-CuNPs and the highest elimination with CRE of 91.8% was achieved in the first 20 min, and then equilibrium was reached. This result suggests that the increasing time leads to increased contact between the CIP molecules and the active sites of GM-CuNPs (*47*). After CIP molecules saturate on the active sites of the nanoparticles, the CRE value does not significantly increase because the particles have reached their full capacity. This result is in agreement with previous reports showing that the removal of antibiotics by CuNPs depends on the adsorption mechanism (*48*).

CIP is a zwitterionic molecule with two pK_as; pK_{a1} of 6.1 and pK_{a2} of 8.7 (*49,50*), which is due to the proton predominance of the amine and carboxylic groups, respectively. The removal of CIP from water using GM-CuNPs was a pH-dependent phenomenon. It was observed that the removal process occurred along with the charge interaction adsorption mechanism. The highest CRE values within 20 min were found in the pH range of approximately 6-7, where the CIP molecule was in its zwitterionic form. In this pH range, CIP molecules possess both negative and positive charges. As a result, the interaction between GM-CuNPs and CIP is maximized. At pH lower than 6 or lower than pK_{a1} of CIP, the solution contained a high amount of H^{+} cation, which completely interacted with the anion of GM-CuNPs. This competition resulted in a decrease in the adsorption of CIP by the active site of GM-CuNPs. At pH greater than 7, the negative salt form of CIP at pK_{a2} was dominant (*51,52*) and was repelled by the negatively charged of GM-CuNPs. Therefore, the adsorption of CIP by GM-CuNPs decreased again in alkaline medium. From these results, it was concluded that the highest removal efficiency of CIP by GM-CuNPs could be obtained only in the optimum pH range of 6-7. In studies on the effects of temperature, it was found that the maximum removal efficiency could only be achieved at appropriate temperature. This can be considered that interaction between CIP molecules and GM-CuNPs is a specific reaction that occurs only at specific temperature. The decreased removal efficiency at temperatures above and below 25-35°C is confirmed to be due to the reduced attraction between the active sites of GM-CuNPs and CIP. In addition, the adsorption efficiency at higher temperatures decreased due to the high mobility of both the adsorbent, GM-CuNPs, and the adsorbate, CIP (*53*). It can be concluded that among the factors studied, pH plays an important role in the CRE of GM-CuNPs. Therefore, it is necessary to adjust the pH to 6-7 before the removal of CIP by this nanoparticle system.

Acknowledgements

The authors are grateful to the Department of Science, Faculty of Science and Agricultural Technology, Rajamangala University of Technology Lanna, Lampang province, Thailand for providing chemical materials. We also would like to thank the Center of Excellence in Pharmaceutical Nanotechnology, Chiang Mai University for the partial support.

Funding: This work was partially supported by Global and Frontier Research University Fund, Naresuan University; Grant number R2566C053 and Agricultural Biochemistry Research Unit, Faculty of Sciences and Agricultural Technology, Rajamangala University of Technology Lanna Lampang.

Conflict of Interest: The authors have no conflicts of interest to disclose.

References

1. Nadia O, Bamfo N, Hosey-Cojocari C, Benet L, Remsberg C. Examination of urinary excretion of unchanged drug in humans and preclinical animal models: Increasing the predictability of poor metabolism in humans. Pharm Res. 2021; 38:1139-1156.
2. Jakobsen L, Lundberg C, Frimodt-Møller N. Ciprofloxacin pharmacokinetics pharmacodynamics against susceptible and low-level resistant escherichia coli isolates in an experimental ascending urinary tract infection model in mice. Antimicrob Agents Chemother. 2020; 65:e01804-e018020.
3. Dewitte B, Dewulf J, Demeestere K, Van De Vyvere V, De Wispelaere P, Van Langenhove H. Ozonation of ciprofloxacin in water: HRMS identification of reaction products and pathways. Environ Sci Technol. 2008; 42:4889-4895.
4. El-Shafey E, Al-Lawati H, Al-Sumri A. Ciprofloxacin adsorption from aqueous solution onto chemically prepared carbon from date palm leaflets. J Environ Sci. 2012; 24:1579-1586.
5. Fick J, Soderstrom H, Lindberg R, Chau Phan C, Tysklind M, Larsson D. Contamination of surface, ground, and drinking water from pharmaceutical production. Environ Toxicol Chem. 2009; 28:2522-2527.
6. Liu W, Sutton NB, Rijnaarts HHM, Langenhoff AAM. Pharmaceutical removal from water with iron- or manganese-based technologies: A review. Crit Rev Environ Sci Technol. 2016; 46:1584-1621.
7. Mohammed AA, Kareem SL. Enhancement of ciprofloxacin antibiotic removal from aqueous solution using zno nanoparticles coated on pistachio shell. Desalin Water Treat. 2021; 213:229-239.
8. He P, Mao T, Wang A, Yin Y, Shen J, Chen H, Zhang, P. Enhanced reductive removal of ciprofloxacin in pharmaceutical wastewater using biogenic palladium nanoparticles by bubbling H_2. RSC Advan. 2020; 10:26067-26077.
9. Reverberi AP, Kuznetsov NT, Meshalkin VP, Salerno M, Fabiano B. Systematical analysis of chemical methods in metal nanoparticles synthesis. Theor Found Chem Eng. 2016; 50:59-66.
10. Haddawi, SF, Humud HR, Hamidi SM. Signature of plasmonic nanoparticles in multi-wavelength low power random lasing. Opt Laser Technol. 2020; 121:105770.
11. Adetuyi F, Karigidi K, Akintimehin E, Adeyemo O. Antioxidant properties of *Ageratum conyzoides* L. Asteraceae leaves. Bangladesh J Sci Ind Res. 2018; 53:265-276.
12. Shylesh BS, Padikkala J. Antioxidant and anti-inflammatory activity of *Emilia sonchifolia*. Fitoterapia 1999; 70:275-278.
13. Shen SM, Shen L, Zhang J, Li G, Li Z, Pan R, Si J. Emiline, a new alkaloid from the aerial parts of *Emilia sonchifolia*. Phytochem Lett. 2013; 6:467-470.
14. Gubbiveeranna V, Nagaraju S. Ethnomedicinal, phytochemical constituents and pharmacological activities of *Tridax procumbens*: A review. Int J Pharm Pharm Sci. 2016; 8:1-7.
15. Guemmaz T, Zerargui F, Boumerfeg S, Arrar L, Aouachria S, Khennouf S, Charef NE, Baghiani A. Anti-hemolytic, anti-lipid peroxidation, antioxidant properties and acute toxicity of *Xanthium strumarium* leaves extracts. Annu Res Rev Biol. 2018; 24:1-12.
16. Sharifi-Rad J, Hoseini-Alfatemi SM, Sharifi-Rad M, Sharifi-Rad M, Iriti M, Sharifi-Rad M, Sharifi-Rad R, Raeisi S. Phytochemical compositions and biological activities of essential oil from *Xanthium strumarium* L. Molecules. 2015; 20:7034-7047.
17. Srinivas P, Rajashekar V, Upender Rao E, Venkateshwarulu L, Anil kumar CH. Phytochemical screening and *in vitro* antimicrobial investigation of the methanolic extract of *Xanthium strumarium* leaf. Int J Drug Dev Res. 2011; 3:286-293.
18. Mohamed G, Al-Abd A, El-Halawany A, Abdallah H, Ibrahim S. New xanthones and cytotoxic constituents from *Garcinia mangostana* fruit hulls against human hepatocellular, breast, and colorectal cancer cell lines. J Ethnopharmacol. 2017; 198:302-312.
19. Veerasamy R, Xin TZ, Gunasagaran S, Xiang TFW, Yang EFC, Jeyakumar N, Dhanaraj SA. Biosynthesis of silver nanoparticles using mangosteen leaf extract and evaluation of their antimicrobial activities. J Saudi Chem Soc. 2011; 15:113-120.
20. Anantaworasakul P, Okonogi S, Klayraung S. Antibacterial activities of *Sesbania grandiflora* extracts. Drug Discov Ther. 2016; 5:1256-1262.
21. Samuel P. Bioefficacy of *Sesbania grandiflora* leaves silver nanoparticles against *Aedes aegypti* larvae. J Adv Sci Res. 2021; 12:176-184.
22. Zhang A, Fang Y, Wang H, Li H, Zhang Z. Free-radical scavenging properties and reducing power of grape cane extracts from 11 selected grape cultivars widely grown in China. Molecules. 2011; 16:10104-10122.
23. Amaliyah S, Pangesti DP, Masruri M, Sabarudin A, Sumitro SB. Green synthesis and characterization of copper nanoparticles using *Piper retrofractum* Vahl extract as bioreductor and capping agent. Heliyon. 2020; 6:e04636.
24. Harshiny M, Iswarya CN, Matheswaran M. Biogenic synthesis of iron nanoparticles using *Amaranthus dubius* leaf extract as a reducing agent. Powder Technol. 2015; 286:744-749.
25. Khumpirapang N, Sassa-Deepaeng T, Suknuntha K, Anuchapreeda S, Okonogi S. Masculinizing effects of chrysin-loaded poloxamer micelles on siamese fighting fish. Vet Sci. 2021; 8:305.
26. Sassa-deepaeng T, Pikulkaew S, Okonogi S. Development of chrysin loaded poloxamer micelles and toxicity evaluation in fish embryos. Drug Discov Ther. 2016; 10:150-155.
27. Iwashina I. The Structure and distribution of the flavonoids in plants. J Plant Res. 2000; 113:287-299.
28. Panche AN, Diwan AD, Chandra S. Flavonoids: An overview. J Nutr Sci. 2016; 5:e47.
29. Khanbabaee K, Ree T. Tannins: Classification and definition. Nat Prod Rep. 2001; 18:641-649.
30. Mutha RE, Tatiya AU, Surana SJ. Flavonoids as natural phenolic compounds and their role in therapeutics: an overview. Futur J Pharm Sci. 2021; 7:25.
31. Gourlay G, Constabel CP. Condensed tannins are inducible antioxidants and protect hybrid poplar against oxidative stress. Tree Physiol. 2019; 39:345-355.
32. Quideau S, Deffieux D, Douat-Casassus C, Pouységu L. Plant polyphenols: Chemical properties, biological

activities, and synthesis. Angew Chem Int Edit. 2011; 50:586-621.
33. Gutiérrez-Grijalva EP, Ambriz-Pére DL, Leyva-López N, Castillo-López RI, Heredia JB. Dietary phenolic compounds, health benefits and bioaccessibility. Arch Latinoam Nutr. 2016; 66:87-100.
34. Aryal S, Baniya MK, Danekhu K, Kunwar P, Gurung R, Koirala N. Total Phenolic content, flavonoid content and antioxidant potential of wild vegetables from western Nepal. Plants (Basel). 2019; 8:96.
35. Suárez-Cerda J, Espinoza-Gómez H, Alonso-Núñez G, Rivero IA, Gochi-Ponce Y, Flores-López LZ. A green synthesis of copper nanoparticles using native cyclodextrins as stabilizing agents. J Saudi Chem Soc. 2017; 21:341-348.
36. Amjad R, Mubeen B, Ali SS, Imam SS, Alshehri S, Ghoneim MM, Alzarea SI, Rasool R, Ullah I, Nadeem MS, Kazmi I. Green synthesis and characterization of copper nanoparticles using *Fortunella margarita* leaves. Polymers (Basel). 2021; 13:4364.
37. Mathur A, Kushwaha A, Dalakoti V, Dalakoti G, Singh DD. Green synthesis of silver nanoparticles using medicinal plant and its characterization. Der Pharm Lett. 2014; 5:118-122.
38. Wu S, Rajeshkumar S, Madasamy M, Mahendran V. Green synthesis of copper nanoparticles using *Cissus vitiginea* and its antioxidant and antibacterial activity against urinary tract infection pathogens. Artif Cells Nanomed B. 2020; 48:1153-1158.
39. Ashtaputrey SD, Ashtaputrey PD, Yelane N. Green synthesis and characterization of copper nanoparticles derived from *Murraya koenigii* leaves extract. J Chem Pharm Sci. 2017; 10:1288-2291.
40. Sankar R, Manikandan P, Malarvizhi V, Fathima T, Shivashangari KS, Ravikumar V. Green synthesis of colloidal copper oxide nanoparticles using *Carica papaya* and its application in photocatalytic dye degradation. Spectrochim Acta A. 2014; 121:746-750.
41. Manikandan A, Sathiyabama M. Green synthesis of copper-chitosan nanoparticles and study of its antibacterial activity. J Nanomed Nanotechnol. 2015; 6:1-5.
42. Narayanan M, Jahier-Hussain FA, Srinivasan B, Sambantham MT, Al-Keridis LA, AL-Mekhlafi FA. Green synthesizes and characterization of copper-oxide nanoparticles by *Thespesia populnea* against skin-infection causing microbes. J King Saud Univ-Sci. 2022; 34:101885.
43. Alhalili Z. Green synthesis of copper oxide nanoparticles CuO NPs from *Eucalyptus globoulus* leaf extract: Adsorption and design of experiments. Arab J Chem. 2022; 15:103739.
44. Ijaz F, Shahid S, Khan SA, Ahmad W, Zaman S. Green synthesis of copper oxide nanoparticles using *Abutilon indicum* leaf extract: Antimicrobial, antioxidant and photocatalytic dye degradation activities. Trop J Pharm Res. 2017; 16:743-753.
45. Amaliyah S, Pangesti D, Masruri M, Sabarudin A, Sumitro S. Green synthesis and characterization of copper nanoparticles using *Piper retrofractum* Vahl extract as bioreductor and capping agent. Heliyon 2020; 6:e04636.
46. Balarak D, Mahvi AH, Shim MJ, Lee SM. Adsorption of ciprofloxacin from aqueous solution onto synthesized NiO: Isotherm, kinetic and thermodynamic studies. Desalin Water Treat. 2021; 212:390-400.
47. Abdel-Aziz HM, Farag RS, Abdel-Gawad SA. Carbamazepine removal from aqueous solution by green synthesis zero-valent iron/cu nanoparticles with *Ficus benjamina* leaves' extract. Int J Environ Res. 2019; 13:843-852.
48. Oliveira LMF, Nascimento MA, Guimarães YM, Oliveira AF, Silva AA, Lopes RP. Removal of beta-lactams antibiotics through zero-valent copper nanoparticles. J Braz Chem Soc. 2018; 29:1630-1637.
49. Moradi SE, Haji Shabani AM, Dadfarnia S, Emami S. Effective removal of ciprofloxacin from aqueous solutions using magnetic metal–organic framework sorbents: Mechanisms, isotherms and kinetics. J Iran Chem Soc. 2016; 13:1617-1627.
50. ElShaer A, Ouyang D, Hanson P, Mohammed AR. Preparation and evaluation of amino acid based salt forms of model zwitterionic drug ciprofloxacin. J Pharm Drug Deliv Res. 2013; 2:1-10.
51. Igwegbe CA, Oba SN, Aniagor CO, Adeniyi AG, Ighalo JO. Adsorption of ciprofloxacin from water: A comprehensive review. J Ind Engin Chem. 2021; 93:57-77.
52. El-Bendary N, El-Etriby HK, Mahanna H. Reuse of adsorption residuals for enhancing removal of ciprofloxacin from wastewater. Environ Technol. 2022; 43:4438-4454.
53. Altaf S, Zafar R, Zaman WQ, Ahmad S, Yaqoob K, Syed A, Khan AJ, Bilal M, Arshad M. Removal of levofloxacin from aqueous solution by green synthesized magnetite (Fe_3O_4) nanoparticles using *Moringa olifera*: Kinetics and reaction mechanism analysis. Ecotoxicol Environ Saf. 2021; 226:112826.

Received August 4, 2023; Revised October 3, 2023; Accepted October 8, 2023.

*Address correspondence to:
Siriporn Okonogi, Center of Excellence in Pharmaceutical Nanotechnology, Faculty of Pharmacy, Chiang Mai University, Chiang Mai, Thailand 50200.
E-mail: okng2000@gmail.com

Released online in J-STAGE as advance publication October 16, 2023.